FOOT PLACEMENT IS NOT CONTROLLED BASED ON ANGULAR MOMENTUM

Simone Berkelmans[1,2], Sjoerd Bruijn[1,2,3] and Maarten Afschrift[1,2]

[1] Department of Human Movement Sciences, Faculty of Behavioral and Movement Sciences, Vrije Universiteit Amsterdam, Amsterdam, The Netherlands

[2] Amsterdam Movement Sciences, Program Rehabilitation and Development, Amsterdam, The Netherlands

[3] Institute for Brain and Behavior Amsterdam, Vrije Universiteit Amsterdam, Amsterdam, the Netherlands

Abstract

This study examined how mediolateral foot placement is controlled following mechanical perturbations that affected either whole-body linear or angular momentum. Predictive foot placement models based on center of mass state alone were compared with models that additionally included whole-body angular momentum to determine whether whole-body angular momentum contributes to foot-placement control beyond linear momentum. Ten healthy adults walked on a treadmill at 2 km/h and 5 km/h while exposed to two perturbation types: (1) a pull to the pelvis that primarily altered linear momentum (translation perturbation) and (2) simultaneous pulls to the pelvis and shoulder in opposite directions that primarily altered angular momentum (rotation perturbation). Perturbations were applied at heel strike, with a magnitude of ~120 N and a duration of 300 ms. Whole-body kinematics were recorded using 3D motion capture and processed in OpenSim to compute linear and angular momentum. Translation perturbations caused large deviations in whole-body linear momentum with minimal changes in whole-body angular momentum, whereas rotation perturbations induced strong whole-body angular momentum deviations with smaller changes in linear momentum. Including whole-body angular momentum minimally improved foot-placement predictions during early swing after rotation perturbations. These findings indicate that mediolateral foot placement is primarily governed by linear momentum dynamics.

Key words: Gait stability, Foot placement, Whole-body angular momentum

Introduction

In human walking, the control of linear momentum, particularly that of the center of mass (CoM) motion with respect to the stance foot, has been extensively studied. Humans regulate center of mass motion by modulating the ground reaction force, which, aside from gravity, is the only external force acting on the body (Hof, 2007; Reimann et al., 2018; Winter, 1995). This modulation occurs both through stance-phase strategies, such as ankle and hip torque, and through foot placement (Bauby & Kuo, 2000; Bruijn & Van Dieën, 2018; MacKinnon & Winter, 1993; Reimann et al., 2019; Townsend, 1985). Empirical studies have shown that foot placement location is closely related to the CoM's position and velocity at

mid-stance (Van Den Bogaart et al., 2020; Vlutters et al., 2016; Wang & Srinivasan, 2014). During steady-state gait, muscle activity and the resulting ground reaction force vectors are finely tuned to stabilize the CoM trajectory and maintain balance (Hof & Duysens, 2018; Reimann et al., 2019). This relationship, between CoM dynamics and foot placement, has been formalized through the concept of the extrapolated Center of Mass (XCoM), which combines the instantaneous CoM position and velocity with the dynamics of an inverted pendulum model (Bruijn et al., 2013; Hof, 2007; Hof et al., 2005). The XCoM framework has successfully estimated step width and foot placement adjustments, providing insight into how humans anticipate and correct for potential instability in the sagittal (and frontal) plane (Bruijn & Van Dieën, 2018; O'Connor & Kuo, 2009; Van Mierlo et al., 2022).

In addition to linear momentum, control of angular momentum about the CoM (throughout the manuscript defined with respect to the whole-body center of mass) is a requirement for stable walking (Herr & Popovic, 2008; Van Dieën et al., 2025). While linear momentum provides information about the translation of the body, it does not capture the rotational dynamics of the body. Both linear and angular momentum are determined by external forces, primarily gravity and ground reaction forces, with the latter modulated through stance-phase ankle torques and foot placement (Reimann et al., 2019; Van Den Bogaart et al., 2020). Since gravity is constant, humans achieve this control by adjusting the magnitude, direction, and point of application of ground reaction forces to maintain a stable, periodic gait (Herr & Popovic, 2008; Hof, 2007).

Although foot placement is often viewed as a mechanism to modulate the ground reaction force for controlling the motion of the CoM (Bruijn & Van Dieën, 2018; Van Den Bogaart et al., 2020), Leestma et al. (2023) found that step placement adjustments is also correlated with variations in integrated whole-body angular momentum, particularly in the frontal plane. Complementing this, Van Dieën et al. (2025) proposed that humans use simultaneous feedback control of linear and angular momentum during walking, implying that foot placement is also used to control angular momentum. These findings suggest that foot placement is shaped by the combined need to regulate both linear and angular momentum, rather than linear momentum alone.

Experimental evidence indicates that, under certain conditions, humans prioritize the control of angular over linear momentum. For instance, Pijnappels et al. (2004) showed that following a trip, humans often first control trunk rotation and restore whole-body angular momentum at the cost of deviations in center of mass velocity, highlighting the prioritization of controlling angular momentum. Similarly, Van Mierlo et al. (2022) demonstrated that responses to angular momentum perturbations occur substantially faster than responses to linear perturbations in the sagittal plane. These findings underscore that in challenging situations angular momentum regulation is not only an integral part of locomotor control but can also dominate stability strategies.

While previous work has established that foot placement is tightly coupled to the CoM state and can be well predicted by models such as the XCoM (Hof, 2007; Vlutters et al., 2016; Wang &

Srinivasan, 2014), it remains less clear whether this relationship fully captures how humans control stability when whole-body angular momentum is perturbed. In the present study, we investigated how foot placement is controlled following mechanical perturbations that selectively affected either CoM motion (translation perturbations) or whole-body angular momentum (rotation perturbations). By comparing predictive models based on CoM state alone with models that additionally included whole-body angular momentum, we aimed to determine whether whole-body angular momentum contributes to the control of mediolateral foot placement beyond linear CoM dynamics.

Methods

Participants

Fourteen healthy participants (four men; weight 69.6 ± 10.2 kg, height 1.72 ± 0.06 m, mean ± SD) participated in the study. Four participants were excluded due to missing marker data or missing load cell data, resulting in ten participants being included in the analysis. Exclusion criteria were any sports injuries or musculoskeletal conditions that could affect walking patterns or balance, as these could influence the results. The study was approved by the local ethics committee (VCWE-2024-065), and all participants provided written informed consent prior to participation.

Measurement setup and data collection

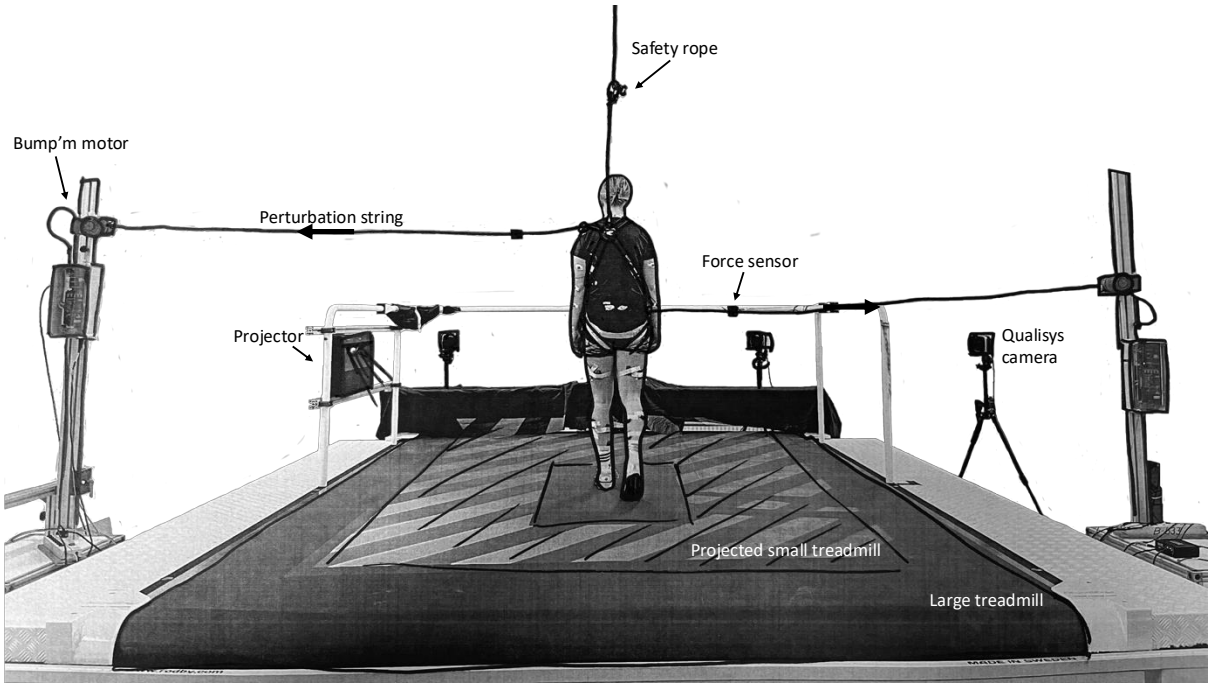

Figure 1: Measurement setup.

Participants walked on a large treadmill (250 cm × 450 cm; Rodby innovation, RL4500E, Sweden; Figure 1). A projector displayed the outline of a standard-size treadmill (75 cm × 200 cm) onto the large treadmill surface, creating a "small treadmill" within the larger belt area. For the present study, only

perturbations on the large treadmill were analyzed. Participants wore a full-body safety harness attached to an overhead safety rope to prevent injury in case of a fall and to ensure they would not contact the treadmill surface.

Mechanical perturbations were applied using two motors (Bump'm; Tan et al., 2020). The right motor was mounted approximately 75 cm above the treadmill base, aligned with the participant's pelvis, to deliver right-lateral pulls. The left motor was mounted approximately 150 cm above the treadmill base, aligned with the left shoulder, to deliver left-lateral pulls. Each motor was connected to the harness via perturbation strings attached at the right pelvis and left shoulder, respectively. A force sensor (Avanti Load Cell Adapter, Delsys Inc. Natick, MA, USA; sampling frequency 2000 Hz) was in-line with each perturbation string to record the applied loads.

Seven Qualisys Argus cameras (Qualisys, Göteborg, Sweden; sampling frequency 100 Hz) captured full-body kinematics. Reflective markers were placed on anatomical landmarks and cluster locations (Supplementary Material, Table S1), including the harness and perturbation strings to track the applied forces.

All systems were synchronized using a 5V pulse from the Qualisys sync unit.

Experimental protocol

All participants walked on the treadmill at two speeds: slow (2 km/h) and normal (5 km/h). Prior research has shown that deviations in CoM state and deviations in foot placement might be speed dependent, which is particularly relevant for clinical populations such as individuals with spinal cord injury (SCI), who often walk at significantly reduced speeds (Zadravec et al., 2020). The experiment was divided into two blocks (slow and normal walking), with all participants starting with the slow walking condition. Within each block, participants walked on both the large and the projected small treadmill, with the order of treadmill type randomized across participants. Participants were instructed to respond to perturbations by regaining balance and returning to their original position on the treadmill.

Before starting the first block, participants completed a five-minute familiarization period to adjust to walking on the treadmill as well as to the safety harness and string attachment. During this period, they walked at both walking speeds.

Perturbations were applied either as a force to the pelvis alone or as rotation perturbation involving simultaneous forces to both the pelvis and shoulder (Figure 2A and B). The rotation perturbation generated a moment on the torso without producing a net linear force (see Figure 2C). Each block included four perturbation conditions: Translation Right, which was a right pelvis pull applied at initial contact of the right leg; Translation Left, a right pelvis pull at initial contact of the left leg; Rotation Right, a combined pull on the right pelvis and left shoulder at initial contact of the right leg; and Rotation Left, the same combined pull applied at initial contact of the left leg. Each perturbation was an impulse lasting 300 ms with a force magnitude of ±120 N, comparable to the strongest perturbations used in Van Mierlo et al. (2022). Each condition was repeated 10 times per block, resulting

in a total of 160 perturbations across the entire experiment. Perturbations were delivered at random intervals ranging from 8 to 12 seconds to avoid anticipation.

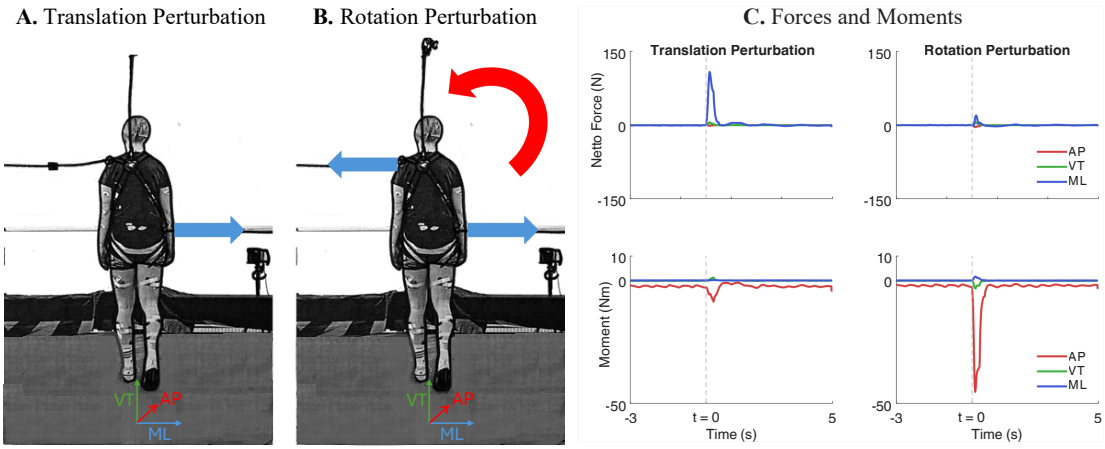

Figure 2: (A) Translation perturbation, applied as a pull (blue arrow) to the pelvis (right); (B) Rotation perturbation, applied as simultaneous pulls (blue arrows) to both the pelvis (right) and shoulder (left), with the resulting moment about the CoM (red arrow); (C) Forces (top panels) and moments about the CoM (bottom panels) during translation (pelvis) and rotation (pelvis–shoulder) perturbations, plotted with perturbation onset at t = 0, including 3 seconds prior and 5 seconds following the perturbation. AP: anterior-posterior, ML: mediolateral, and VT: vertical.

Data processing

Raw marker data from Qualisys were labeled in QTM-software. The marker trajectories, load cell signals, surface EMG, and perturbation data were preprocessed in Python (Python, version 3.12). For each participant, trials were synchronized across the Qualisys motion capture, load cell recordings, surface EMG, and Bump'm system. All trial data were time-normalized relative to the perturbation onset ($t = 0$). For each trial, three seconds of data prior and five seconds following the perturbation were extracted for analysis.

Gait events were detected from heel and toe marker trajectories (low-pass filtered with a second-order Butterworth, cut off 4 Hz). Heel strikes were identified by locating downward peaks in the vertical velocity of the heel marker and then selecting the first frame after each peak at which the heel vertical velocity returned to approximately zero, corresponding to foot contact. Toe-offs were defined as the first frame after each heel strike at which the anterior-posterior velocity of the toe marker, corrected for treadmill speed, exceeded a predefined threshold. Default thresholds were 0.05 $m \cdot s^{-1}$ for both the heel vertical and toe anterior-posterior velocities unless otherwise specified.

We scaled the generic Gait2392 musculoskeletal model in OpenSim (version 4.5) to each participant based on individual anthropometry and body mass. The scaled model, together with the processed marker trajectories, was used for inverse kinematics to compute joint angles. From these

analyses, segment orientations and whole-body CoM positions and velocities were derived. Whole-body angular momentum was calculated following Herr & Popovic, (2008):

$$\vec{H} = \sum_{i=1}^{N} [\,(\vec{r}_i - \vec{r}_{CoM}) \times m_i(\vec{v}_i - \vec{v}_{CoM}) + I_i\vec{\omega}_i]$$

Where i represents each body segment of the OpenSim model, r_i and r_{CoM} are the positions of the ith segment CoM and the whole-body CoM, respectively v_i and v_{CoM} are the velocities of the ith segment and the whole-body CoM, m_i is the mass of the ith segment, I_i is the segment's inertia tensor, and ω_i is the angular velocity of the ith segment's CoM (Herr & Popovic, 2008).

Outcome measures

Step width, *step time*, and *margin of stability* were analyzed for the final unperturbed step (Pre) and the first three steps following the perturbation (Post 1–Post 3). *Step width* was defined as the mediolateral distance between left and right heel markers at heel strike. *Step time* was defined as the temporal interval between heel strikes of alternating feet. Mediolateral *XCoM* was computed according to Hof (2007):

$$XCoM = \mathrm{r}_{ML,CoM} + \frac{v_{ML,CoM}}{\sqrt{g/l}}$$

Where $r_{ML,CoM}$ is the mediolateral CoM position, $v_{ML,CoM}$ is the mediolateral CoM velocity, $g = 9.81\ ms^{-2}$, and l is the effective pendulum length approximated by the mean vertical CoM height (Hof, 2007). The *margins of stability* in the mediolateral direction was then calculated as the distance between the XCoM and the position of the leading foot at toe-off of the trailing foot. A positive margin of stability indicates that the XCoM lies within the base of support.

Mediolateral foot placement was estimated using linear regression models to evaluate if foot placement is related to preceding mediolateral CoM position ($r_{ML,CoM}$) and velocity ($v_{ML,CoM}$) with respect to the stance foot, and whole-body angular momentum. CoM position and velocity relative to the stance foot were denoted as $r^{rel}_{ML,CoM}$ and $v^{rel}_{ML,CoM}$, respectively.

Model 1 only included CoM position and velocity as predictors:

$$1.\,Foot\ placement = \beta_0 + \beta_1\, r^{rel}_{ML,CoM} + \beta_2 v^{rel}_{ML,CoM} + \varepsilon$$

Model 2 additionally included whole-body angular momentum as a predictor:

$$2.\,Foot\ placement = \beta_0 + \beta_1\, r^{rel}_{ML,CoM} + \beta_2 v^{rel}_{ML,CoM} + \beta_3 WBAM_z + \varepsilon$$

Regressions models 1 and 2 were fitted ($\beta_0, \beta_1, \beta_2, \beta_3$) using the least squares procedure on data from rotation and translation perturbations. The data set included all steps in the time window of three seconds prior and five seconds following the perturbation onset. By comparing these two models, we aimed to assess how much the additional variance in foot placement is explained when whole-body angular momentum is included alongside CoM kinematics. Model performance was assessed using

regression coefficients, relative explained variance (R^2), and step-by-step prediction errors (residuals, ε).

Statistics

Step time, step width, and *margin of stability* were analyzed for the final unperturbed step (Pre) and the first three steps following the perturbation (Post 1–Post 3). Separate paired t-tests, or non-parametric equivalent, were performed to compare Pre vs. Post 1, Pre vs. Post 2, and Pre vs. Post 3. This approach was chosen to directly assess how *step time, step width,* and *margin of stability* changed following perturbation exposure, without modeling complex interactions across perturbation types or walking speeds. Walking speed and perturbation type were not included, as the primary interest was in the recovery steps rather than between-perturbation differences. The significance level was set at $\alpha = 0.05$, and p-values were Bonferroni-corrected for multiple comparisons.

Results

During translation perturbations, both CoM position and velocity showed substantial deviations from unperturbed steps (see Figure 3), with mediolateral CoM displacements (~0.2 m) and increases in velocity (up to ~0.4 m/s). Whole-body angular momentum remained mostly unchanged compared with unperturbed steps, with some slight deviations in the first two post-perturbation steps. These responses were similar between walking speeds. Rotational perturbations caused clear whole-body angular momentum deviations (up to ~5 kg m^2/s). CoM position and velocity also deviated from unperturbed trajectories (~0.05 m), although to a smaller extent than during translation perturbations, especially during the first two post-perturbation steps. Faster walking amplified the whole-body angular momentum response and slightly increased CoM position and velocity deviations relative to slow walking.

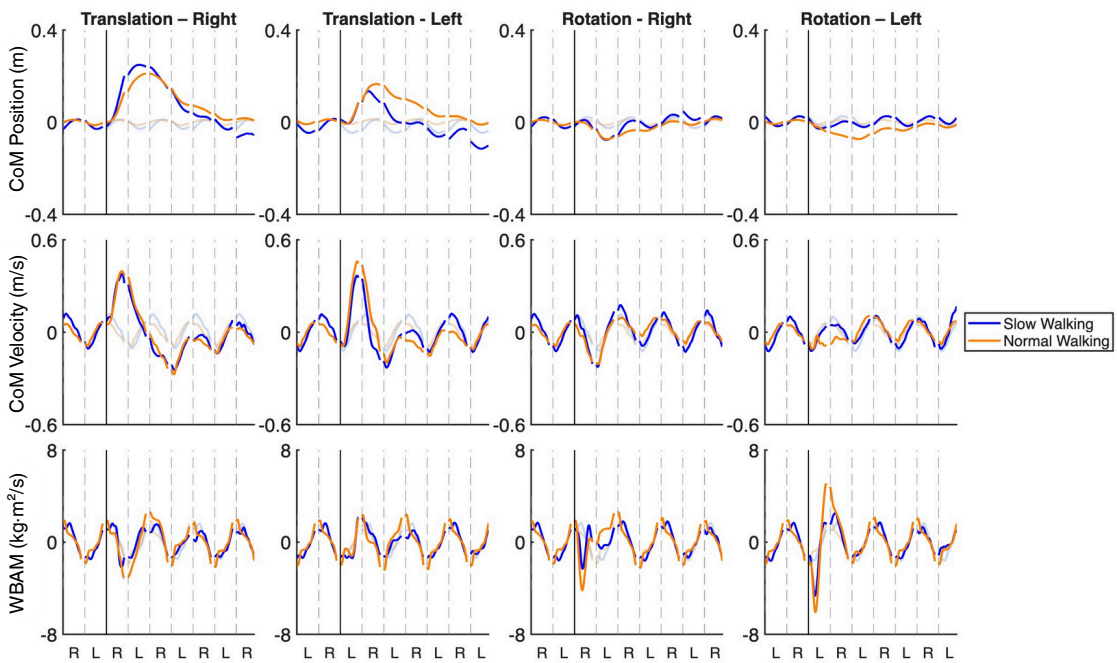

Figure 3: Mediolateral CoM position (top row), CoM velocity (middle row), and whole-body angular momentum (bottom row) across steps for different perturbation types. Columns correspond to perturbation types: Translation Right, Translation Left, Rotation Right, Rotation Left. Blue and orange lines indicate slow and normal walking speed, respectively, with lighter grey shades representing unperturbed steps. Heel strikes are denoted by R (right) and L (left); intervals from R to L indicate right stance, and from L to R indicate left stance. The solid vertical line marks the onset of the perturbation, and dashed vertical lines indicate subsequent heel strikes.

Step time

Perturbations affected step time (Figure 4A) during both slow and normal walking. In general, the first post-perturbation step was shorter, indicating an immediate adjustment in step duration. For translation perturbations, this shorter step occurred regardless of walking speed, whereas for rotational perturbations, the effect was more variable depending on the direction and speed. After this initial adjustment, step time quickly returned to normal for all perturbation types.

Step width

Perturbations affected step width (Figure 4B) during both slow and normal walking. In general, participants first stepped in the direction of the perturbation/applied pull (Post 1). For translation perturbations, this meant stepping toward the side to which the pull displaced the body, and for rotational perturbations, stepping in the direction of the body's induced rotation (Figure 2 and 3). Depending on the stance leg at perturbation onset, this resulted in an outward/wider step width (Perturbations: Translation Left, Rotation Right) or a cross over/smaller step width (Perturbations: Translation Right, Rotation Left). For translation perturbations, the second step (Post 2) was also in the

direction of the perturbation whereas for rotational perturbation the step width was in general normal again.

Margins of stability

Perturbations affected mediolateral margins of stability (Figure 5C) during both slow and normal walking. The margins of stability decreased toward the stance limb during the perturbed step (Post 1), reflecting a shift of the XCoM toward that side. For translation perturbations, the lateral pull displaced the body and reduced margins of stability on the side of the pull. For rotational perturbations, the whole-body rotation similarly shifted the XCoM toward the direction of rotation, producing a comparable margins of stability reduction. The direction of the margins of stability change depended on which foot was in stance at perturbation onset, resulting in either an outward margins of stability shift (Translation Left, Rotation Right) or an inward margins of stability shift (Translation Right, Rotation Left). Following translation perturbations, the margins of stability often remained reduced, or in some cases over-corrected, into the second and third step (Post 2 and 3), likely because participants attempted to return to their original location on the treadmill. In contrast, margins of stability returned to baseline more rapidly after rotational perturbations, possibly due to their smaller effect on CoM displacement and velocity (i.e., smaller initial XCoM deviations). These margins of stability changes were larger during normal walking compared to slow walking.

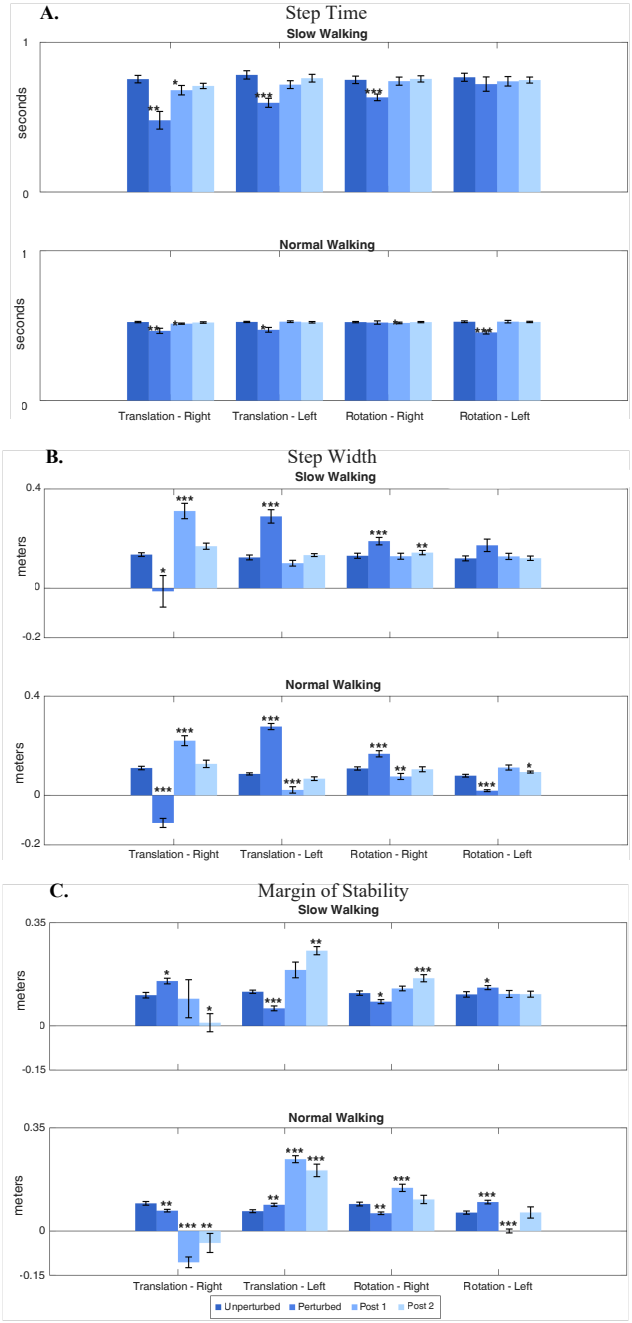

*Figure 4: (A) Step time, (B) Step width, and (C) Margins of Stability during slow and normal walking after translation and rotation perturbations. Different colored bars show group mean ± SD for the unperturbed step (Unperturbed) and the first three post-perturbation steps (Post 1–3) for each perturbation type (Translation Right, Translation Left, Rotation Right, and Rotation Left). * $p < 0.05$; ** $p < 0.01$; *** $p < 0.001$.*

Foot placement

For rotation perturbations, models that included whole-body angular momentum as a predictor (figure 5A, solid red lines) showed a slightly higher R^2 values during the first half of the swing phase, indicating improved model performance when whole-body angular momentum was included. However, in the

second half of the swing phase, the difference between models with and without whole-body angular momentum was negligible. For translation perturbations, the inclusion of whole-body angular momentum (figure 5A, solid purple lines) did not substantially improve model performance, as R^2 values remained similar to those of models without whole-body angular momentum (dashed purple lines) throughout the swing phase. This is also reflected in Figure 5A, where the coefficient values of whole-body angular momentum (β_3) are plotted. This suggests that whole-body angular momentum plays a limited and time-specific role, primarily during early swing under rotational instability, and its contribution to foot placement adjustments is largely negligible during slow walking and translational perturbations.

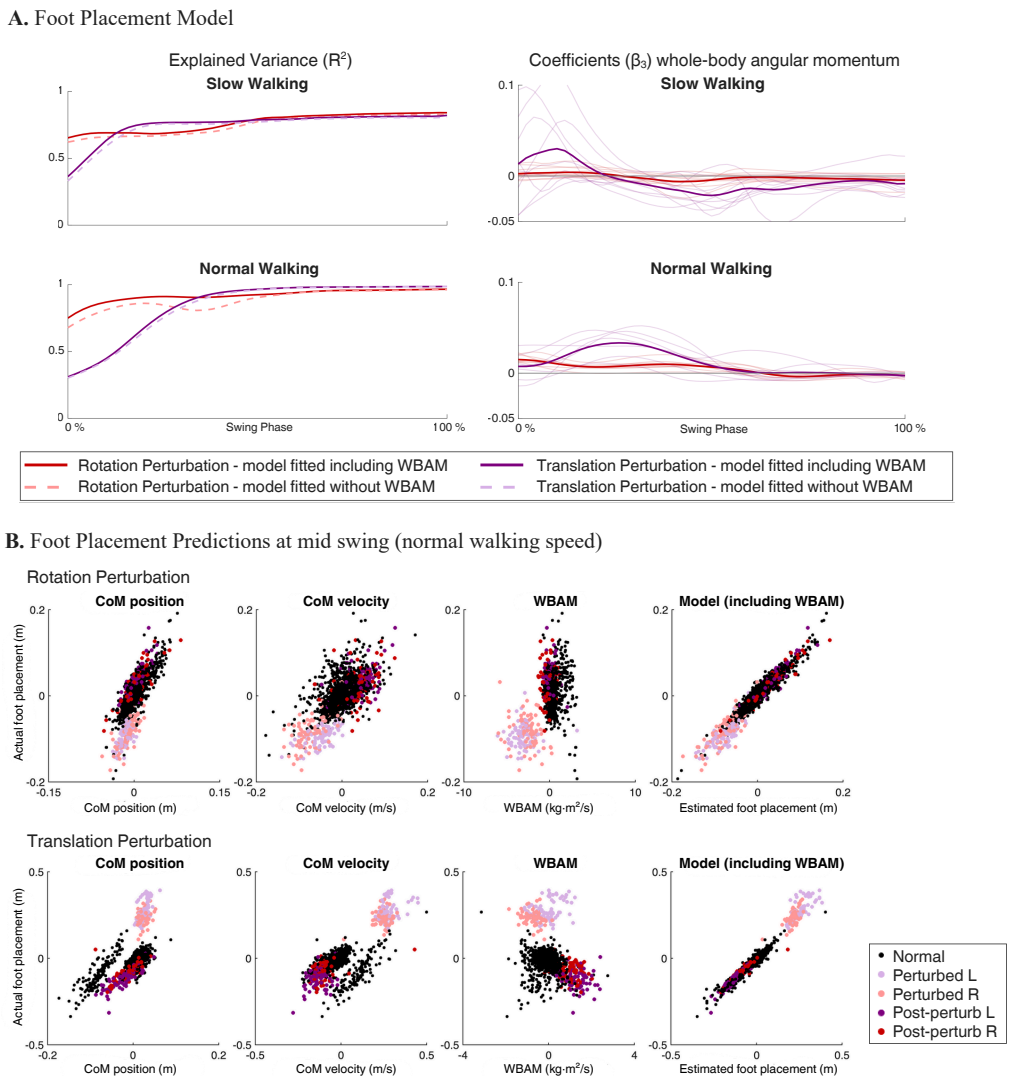

Figure 5: (A) Explained variance (R^2; left figure) and regression coefficient whole-body angular momentum (right figure) during the swing phase for mediolateral foot placement models for slow and normal walking speed. Model performance is shown for translation (purple) and rotation (red) perturbations, for models excluding whole-body angular momentum as a predictor (dashed lines, foot placement model 1), and including whole-body angular momentum as a predictor (solid lines, foot placement model 2). (B) Foot placement (estimated by the regression model including whole-body

angular momentum) and actual foot placement at mid swing for regression coefficients CoM position, CoM velocity, whole-body angular momentum (WBAM), and model 2 (methods, model including whole-body angular momentum).

Discussion

We investigated how foot placement is controlled following perturbations that affected either CoM linear momentum (translation perturbations) or whole-body angular momentum (rotation perturbations). We did so by comparing models which estimated deviations in foot placement based on CoM state alone with models that additionally included whole-body angular momentum. We found that foot placements models that included whole-body angular momentum as a predictor (figure 5A, solid red lines) only slightly increase the explained variance compared to models with only CoM kinematic information (Supplementary Figures S1–S12 and stable model coefficients in S14). This indicate that mediolateral foot placement primarily is coordinated with respect to CoM linear momentum, while whole-body angular momentum plays a limited role.

Contrary to our initial hypothesis, deviations in whole-body angular momentum explained only a small additional portion of the variance in foot placement, even in response to angular momentum perturbations. Participants appeared to restore whole-body angular momentum to near steady-state values during the perturbed stance phase, likely through modulations of mediolateral ground reaction forces. These forces may have originated from active muscle responses (e.g., hip abductors/adductors) or passive skeletal mechanics, which would also explain the small but consistent deviations in mediolateral CoM kinematics (observed after rotational perturbations, Figure 3 and Supplementary Figures S1–S12). Rotational disturbances inevitably create small translational CoM effects due to inverted pendulum mechanics and redirection of the ground reaction force. Such early whole-body angular momentum corrections are consistent with observations by Van Mierlo et al., (2022, 2023), who showed that whole-body angular momentum stabilization occurs very early after a disturbance and is driven largely by re-direction of the ground reaction force rather than by substantial center of pressure shifts. Their work also demonstrated that individuals prioritize restoring whole-body orientation before addressing translational CoM deviations, a pattern that strongly aligns with the small but systematic mediolateral CoM disturbances we observed following rotational perturbations.

The early restoration of whole-body angular momentum likely explains why including whole-body angular momentum improved foot-placement predictions only during early swing in our data. Once whole-body angular momentum is sufficiently regulated during stance, the remaining control effort likely focuses on re-establishing CoM stability through appropriate foot placement. The relatively small contribution of whole-body angular momentum to foot-placement modulation contrasts with findings from Leestma et al. (2023), who reported stronger whole-body angular momentum step-placement relationships, particularly in the frontal plane. These differences may reflect methodological factors: Leestma et al. (2023) perturbed participants later in stance and used integrated whole-body

angular momentum over the full step, which masks in-stance corrections. In contrast, our perturbations were applied early, allowing participants to correct whole-body angular momentum before needing to adjust foot placement, thereby diminishing its apparent predictive value. Given this, perturbations delivered later in stance (e.g., mid-stance or terminal stance) may have prevented the rapid in-stance correction of whole-body angular momentum observed in our data, and whole-body angular momentum might then have explained a larger portion of foot-placement variance. Leestma et al. (2023) used a treadmill translation as a perturbation which might result in a different perturbation magnitude and deviations in linear and angular momentum. Stronger perturbations may have elicited more pronounced responses, potentially impacting foot placement more significantly.

Real-life implications

These findings have potential implications for the design of biomimetic controllers and assistive devices, such as exoskeletons or functional electrical stimulation systems for individuals with spinal cord injury. Understanding the coupling between whole-body angular momentum and foot placement can inform control strategies that stabilize gait and improve balance. For instance, timing and magnitude of perturbation responses could guide adaptive stimulation patterns to prevent falls. Additionally, insights into how the body corrects for perturbations may help optimize predictive control in exoskeletons to support natural, efficient walking. Incorporating such dynamics could enhance safety and functional mobility for users in real-world environments.

Conclusions

Foot placement is predominantly correlated with linear momentum, and only to a limited extend with whole-body angular momentum following both translation and rotation perturbations. Our results indicate that rotational deviations are corrected rapidly within the stance phase, and that subsequent foot placement is used to control linear momentum. Incorporating both translational and rotational feedback may be beneficial for rehabilitation, robotic gait, and exoskeleton design, but translational CoM information remains the primary driver of mediolateral foot placement.

Acknowledgements

Simone Berkelmans was supported by the Netherlands Organization for Scientific Research (NWO), grant OCENW.XS23.1.143**.** The authors would like to thank Lars van Rikxoord for his valuable assistance during this project. We also thank Richard Casius and Bert Clairbois for their support with the measurement (“bump’m”) system throughout the study.

References

Bauby, C. E., & Kuo, A. D. (2000). Active control of lateral balance in human walking. *Journal of Biomechanics*, *33*(11), 1433–1440. https://doi.org/10.1016/S0021-9290(00)00101-9

Bruijn, S. M., Meijer, O. G., Beek, P. J., & Van Dieën, J. H. (2013). Assessing the stability of human locomotion: A review of current measures. *Journal of The Royal Society Interface*, *10*(83), 20120999. https://doi.org/10.1098/rsif.2012.0999

Bruijn, S. M., & Van Dieën, J. H. (2018). Control of human gait stability through foot placement. *Journal of The Royal Society Interface*, *15*(143), 20170816. https://doi.org/10.1098/rsif.2017.0816

Freriks, B., Hermens, H. J., & European Commission Biomedical and Health Research Programme. (2000). *European recommendations for Surface ElectroMyography: Results of the SENIAM Project*. Roessingh Research and Development; WorldCat.

Herr, H., & Popovic, M. (2008). Angular momentum in human walking. *Journal of Experimental Biology*, *211*(4), 467–481. https://doi.org/10.1242/jeb.008573

Hof, A. L. (2007). The equations of motion for a standing human reveal three mechanisms for balance. *Journal of Biomechanics*, *40*(2), 451–457. https://doi.org/10.1016/j.jbiomech.2005.12.016

Hof, A. L., & Duysens, J. (2018). Responses of human ankle muscles to mediolateral balance perturbations during walking. *Human Movement Science*, *57*, 69–82. https://doi.org/10.1016/j.humov.2017.11.009

Hof, A. L., Gazendam, M. G. J., & Sinke, W. E. (2005). The condition for dynamic stability. *Journal of Biomechanics*, *38*(1), 1–8. https://doi.org/10.1016/j.jbiomech.2004.03.025

Leestma, J. K., Golyski, P. R., Smith, C. R., Sawicki, G. S., & Young, A. J. (2023). Linking whole-body angular momentum and step placement during perturbed human walking. *Journal of Experimental Biology*, *226*(6), jeb244760. https://doi.org/10.1242/jeb.244760

MacKinnon, C. D., & Winter, D. A. (1993). Control of whole body balance in the frontal plane during human walking. *Journal of Biomechanics*, *26*(6), 633–644. https://doi.org/10.1016/0021-9290(93)90027-C

O'Connor, S. M., & Kuo, A. D. (2009). Direction-Dependent Control of Balance During Walking and Standing. *Journal of Neurophysiology*, *102*(3), 1411–1419. https://doi.org/10.1152/jn.00131.2009

Pijnappels, M., Bobbert, M. F., & Van Dieën, J. H. (2004). Contribution of the support limb in control of angular momentum after tripping. *Journal of Biomechanics*, *37*(12), 1811–1818. https://doi.org/10.1016/j.jbiomech.2004.02.038

Reimann, H., Fettrow, T., Grenet, D., Thompson, E. D., & Jeka, J. J. (2019). *The onset time of balance control during walking is phase-independent, but the magnitude of the response is not*. Neuroscience. https://doi.org/10.1101/655928

Reimann, H., Fettrow, T., & Jeka, J. J. (2018). Strategies for the Control of Balance During Locomotion. *Kinesiology Review*, *7*(1), 18–25. https://doi.org/10.1123/kr.2017-0053

Tan, G. R., Raitor, M., & Collins, S. H. (2020). Bump'em: An Open-Source, Bump-Emulation System for Studying Human Balance and Gait. *2020 IEEE International Conference on Robotics and Automation (ICRA)*, 9093–9099. https://doi.org/10.1109/ICRA40945.2020.9197105

Townsend, M. A. (1985). Biped gait stabilization via foot placement. *Journal of Biomechanics*, *18*(1), 21–38. https://doi.org/10.1016/0021-9290(85)90042-9

Van Den Bogaart, M., Bruijn, S. M., Van Dieën, J. H., & Meyns, P. (2020). The effect of anteroposterior perturbations on the control of the center of mass during treadmill walking. *Journal of Biomechanics*, *103*, 109660. https://doi.org/10.1016/j.jbiomech.2020.109660

Van Dieën, J. H., Bruijn, S., Lemaire, K. K., & Kistemaker, D. A. (2025). *Simultaneous stabilizing feedback control of linear and angular momentum in human walking*. Biophysics. https://doi.org/10.1101/2025.01.09.632072

Van Mierlo, M., Abma, M., Vlutters, M., Van Asseldonk, E. H. F., & Van Der Kooij, H. (2023). Effect of perturbation timing on recovering whole-body angular momentum during very slow walking. *Human Movement Science*, *91*, 103138. https://doi.org/10.1016/j.humov.2023.103138

Van Mierlo, M., Ambrosius, J. I., Vlutters, M., Van Asseldonk, E. H. F., & Van Der Kooij, H. (2022). Recovery from sagittal-plane whole body angular momentum perturbations during walking. *Journal of Biomechanics*, *141*, 111169. https://doi.org/10.1016/j.jbiomech.2022.111169

Van Mierlo, M., Vlutters, M., Van Asseldonk, E. H. F., & Van Der Kooij, H. (2023). Sagittal-plane balance perturbations during very slow walking: Strategies for recovering linear and angular momentum. *Journal of Biomechanics*, *152*, 111580. https://doi.org/10.1016/j.jbiomech.2023.111580

Vlutters, M., Van Asseldonk, E. H. F., & Van Der Kooij, H. (2016). Center of mass velocity based predictions in balance recovery following pelvis perturbations during human walking. *Journal of Experimental Biology*, jeb.129338. https://doi.org/10.1242/jeb.129338

Wang, Y., & Srinivasan, M. (2014). Stepping in the direction of the fall: The next foot placement can be predicted from current upper body state in steady-state walking. *Biology Letters*, *10*(9), 20140405. https://doi.org/10.1098/rsbl.2014.0405

Winter, D. (1995). Human balance and posture control during standing and walking. *Gait & Posture*, *3*(4), 193–214. https://doi.org/10.1016/0966-6362(96)82849-9

Zadravec, M., Olenšek, A., Rudolf, M., Bizovičar, N., Goljar, N., & Matjačić, Z. (2020). Assessment of dynamic balancing responses following perturbations during slow walking in relation to clinical outcome measures for high-functioning post-stroke subjects. *Journal of NeuroEngineering and Rehabilitation*, *17*(1), 85. https://doi.org/10.1186/s12984-020-00710-5